MACRO- AND MICRO-STABILITIES OF THE KRINGLE 4 DOMAIN FROM PLASMINOGEN

The Effect of Ligand Binding

ANTONIO DE MARCO, ANDREA MOTTA, MIGUEL LLINÁS, AND RICHARD A. LAURSEN
Department of Chemistry, Carnegie-Mellon University, Pittsburgh, Pennsylvania 15213; and Department of Chemistry, Boston University, Boston, Massachusetts 02215

ABSTRACT ^{1}H-NMR spectra of kringle 4 from human plasminogen have been recorded over wide pH* and temperature ranges, both in the presence and in the absence of *p*-benzylaminesulfonic acid (BASA). Several resonances exhibit chemical shift differences between kringle folded and unfolded forms which are sufficiently well resolved to allow for a determination of equilibrium Van't Hoff enthalpies and entropies for unfolding. The interaction with BASA shifts the kringle unfolding temperature from ~335°K to ~343°K. The pH* range of stability is also wider for the complex than for the free kringle: in the acidic range the pH* of half-unfolding, pH^*_u, is decreased from 2.8 for the unligated polypeptide to ~2.0 in the presence of BASA, while in the basic range pH^*_u shifts from ~10.8 to 11.5. However, in contrast with what is observed at acidic pH*, unfolding at basic pH* leads to irreversible denaturation and exhibits a sharp, order-disorder transition both in the presence and in the absence of ligand. The structural stabilization conferred by the ligand is accompanied by a drastic reduction of the average rate of ^{1}H-^{2}H exchange in ^2H_2O under conditions that preclude a major cooperative unfolding. Thus, macro- and micro-stabilities of kringle domains appear to be highly correlated.

INTRODUCTION

Plasmin, a blood plasma serine protease of M_r ~84,000, derives from plasminogen, a zymogen of M_r ~93,000, by enzymatic cleavage of two peptide bonds. The activation, catalyzed by specific tissue activator(s), results in a protein that is composed of two independent polypeptide chains stretching from residues 77 to 560 and 561 to 790, respectively, linked through two cystine bridges (1–3 and references therein). The light chain of plasmin, M_r ~34,000, carries the catalytic center whose main physiological target substrate is polymerized fibrin. The heavier chain is characterized by a tandem array of five highly homologous domains, known as "kringles", of M_r ~10,000 each (4). It is currently thought that at least some of the kringles are responsible for anchoring plasminogen to the fibrin clot (5, 6). In particular, it is well established that kringles 1 and 4 bind ω-amino acid ligands such as lysine, which suggests a mechanism for the interaction holding plasminogen at the clot (7–10). Kringle 4 (Fig. 1) can be readily isolated from the plasminogen heavy chain by controlled elastase digestion, a procedure that generates the intact fragment in relatively good yields (4). Therefore, the kringle 4 domain of human plasminogen affords a convenient model to study the conformation and dynamics of the homologous kringle structures that are ubiquitous among blood plasma proteases that interact with fibrin (11–14).

In a series of elegant differential scanning calorimetry experiments on plasminogen and isolated kringle-containing subfragments, Castellino and coworkers (15) have shown that kringles behave as thermodynamically independent units. These results have been confirmed and further refined by Privalov and coinvestigators (16, 17). An interesting finding from these studies is that upon complexation with ε-aminocaproic acid, a ligand analog of lysine, the midpoint denaturation transition temperature of kringle 4 is raised from ~331–339°K to ~334–349°K, the variability most likely reflecting the somewhat different experimental conditions followed by the two groups of investigators (15, 17). The enhanced thermal stability induced by the ligand is a macroscopic manifestation of underlying dynamic effects within the molecule. Therefore, it would also be of interest to investigate the gradual changes in the microscopic equilibrium populations that are manifest in the thermal unfolding as monitored by the calorimetry technique. Given its atomic resolution, NMR spectroscopy provides a most suitable tool for relating the two aspects of the phenomenon, which presumably represents a first-order cooperative event (18), and to compare

Dr. De Marco's permanent address is Istituto di Chimica delle Macromolecole, Consiglio Nazionale delle Ricerche, Via E. Bassini 15/A, 20133 Milano, Italy.

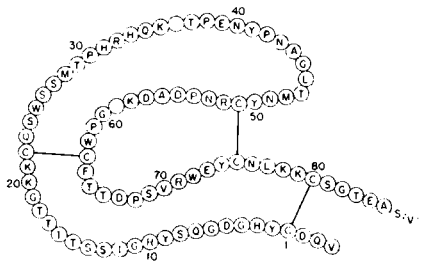

FIGURE 1 Kringle 4 from human plasminogen: outline of the structure. The amino acid sequence (4) is numbered starting from the first half-cystine (Cys^1) so that residues connected towards the NH_2-terminus are labeled with negative numbers or zero. The elastase digestion of the plasminogen heavy chain yields two kringle 4 species that differ in the presence of the -Ser^{86}-Val^{87} COOH-terminus dipeptide (20). The species terminating with Ala^{85} is dominant.

Van't Hoff enthalpies with the macroscopic heat of unfolding.

Structural aspects of kringles from human plasminogen have been studied by ^{1}H-NMR spectroscopy both in our laboratories (19–21) and elsewhere (22). In particular, NMR is most suitable for probing the temperature dependence of conformational unfolding and to detect denaturation. Indeed, the thermal unfolding/refolding of kringle 1 bound to the antifibrinolytic drug *p*-benzylaminesulfonic acid (BASA)[1] has been monitored and shown to be in overall good agreement with differential scanning calorimetry data on kringle 1-containing fragments (19). A second advantage of the high-field NMR approach stems from the atomic level of resolution it affords. As reported previously (20) proton spectroscopy at 600 MHz enables monitoring the time-dependent resonance amplitudes of individual exchange-labile protons of kringles in ^2H_2O solution. This opens the possibility of investigating the extent of ligand-binding effects on the hydrogen-deuterium exchange rates of variously protected (H-bonded, buried, etc.) NH groups. Such exchange kinetics is a most sensitive probe to characterize the local microstability of sites within the kringle structure as opposed to the global macrostability profile provided by the calorimetric studies described above (23).

Here we report a ^{1}H-NMR characterization of the conformational stability of kringle 4 using, among others, a readily detected methionyl S-CH_3^+ singlet to monitor the equilibrium between the globular and open forms. We show that BASA-binding leads to stabilization of the kringle 4 structure against both thermal and acid-base reversible unfoldings and also against the irreversible alkaline denaturation. From the ^{1}H-^{2}H exchange kinetics of individual (peptidyl amide, histidyl imidazole, tryptophanyl indole) NH groups, it is shown that the ligand confers remarkable protection to a large number of such exchange-labile H atoms.

MATERIALS AND METHODS

The kringle 4 samples belonged to batches already described (20, 21). BASA was synthesized by the method of Evans and Milligan (24). Solvent ^2H_2O was purchased from Merck, Sharp & Dohme of Canada, Ltd. Proton NMR spectra were recorded at 300 MHz using a Bruker WM-300 spectrometer (Bruker Instruments, Inc., Billerica, MA) or at 600 MHz at the National NMR Facility for Biomedical Research, Carnegie-Mellon University. Resolution enhancement was achieved via Gaussian convolution (25, 26). Chemical shifts are referred to the 3-trimethylsilyl(2,2,3,3$^2H_4$)propionate signal assumed to appear at −3.766 ppm from dioxane, which was used as internal frequency standard (27). Temperature was checked before and after each experiment with a sample of ethylene glycol.

The analyses of equilibria between folded (f) and unfolded (u) kringle 4 species are based on a two-state model: f ⇌ u. In the case of thermal unfolding (at 1 atm and constant pH)

$$K_u = [u]/[f] = \exp[-\Delta G_u^\circ/RT] = \exp[(T\Delta S_u^\circ - \Delta H_u^\circ)/RT], \quad (1)$$

where K_u is the equilibrium constant for the unfolding process, ΔG_u°, ΔS_u°, and ΔH_u° are the standard unfolding free energy, entropy and enthalpy, respectively, $R = 8.314\ J \cdot K^{-1} \cdot mol^{-1}$ and T is the Kelvin temperature. From Eq. 1 we derive

$$[u]/[K4] = [1 + \exp(\Delta G_u^\circ/RT)]^{-1}, \quad (2)$$

where [K4] = [u] + [f] is the total kringle 4 concentration.

Similarly, for acidic unfolding (at 1 atm and constant temperature) the two-state assumption can be stated as a simple dissociation: $u^+ \rightleftharpoons f + H^+$ where u^+ is a protonated, unfolded form. The proton dissociation equilibrium,

$$K^+ = [f][H^+]/[u^+],$$

where K^+ is the acid dissociation constant, may be expressed as a Henderson-Hasselbach equation:

$$pH = pH_u + \log\{[f]/[u^+]\} \quad (3)$$

which often is modified to

$$pH = pH_u + \log\{[f]/[u^+]\}^{1/s}, \quad (4)$$

where $pH_u = -\log K^+$ is the pH for half-unfolding, i.e., for [f] = [u^+], and s is the Hill coefficient, which may differ from 1 when there is cooperativity (28, and references therein).

From Eq. 4 we obtain the equilibrium constant for unfolding, K_u^+, as a function of pH:

$$K_u^+ = [u^+]/[f] = 10^{-s(pH - pH_u)} \quad (5)$$

so that

$$[u^+]/[K4] = [1 + 10^{s(pH - pH_u)}]^{-1}, \quad (6)$$

where, as above, [K4] = [u^+] + [f]. A similar expression can be derived for alkaline (deprotonation) unfolding at high pH. It should be noted that Eqs. 2 and 6 are formally identical, with

$$\Delta G_u^\circ = 2.303\, sRT\,(pH - pH_u). \quad (7)$$

[1] *Abbreviations used in this paper:* BASA, *p*-benzylaminesulfonic acid; f, folded, native kringle 4; K4, kringle 4; k_{off}, first order rate constant for ligand dissociation; k_{on}, first order rate constant for ligand association; pH*, glass electrode pH reading uncorrected for deuterium isotope effects; pH_u, pH for half-unfolding; ppm, parts per million; $t_{1/2}$, half-life for exchangeable proton; T_u, unfolding temperature; u, unfolded kringle 4.

Therefore, both thermal and acid-base unfolding curves are expected to exhibit similar sigmoidal shapes when plotted against the relevant variables (see Results). In particular, from Eq. 5,

$$\log K_u^+ = s\mathrm{pH}_u - s\mathrm{pH}, \quad (8)$$

so that a plot of log K_u^+ vs. pH is expected to be linear, yielding s (slope) and $s\mathrm{pH}_u$ (intersect). Eq. 8 is formally analogous to the Van't Hoff plot of ln K_u vs. T^{-1} to derive ΔH_u° and ΔS_u°, as indicated by Eq. 1.

The NH hydrogen-exchange rates were determined by measuring the time-dependent resonance intensities as the hydrogen atoms underwent replacement by deuterium. The estimated error on the measured intensities was ±15%. The intensities of the peaks were plotted semilogarithmically vs. time and the exchange rates calculated by linear least-squares fits, assuming first order kinetics (29). No deviation from the exponential decay was observed within the experimental uncertainties. For overlapping resonances the individual rates constants were evaluated by fitting the points with a number of exponentials equal to the number of protons, as evaluated by the integral.

RESULTS

The complete ^{1}H-NMR spectrum of kringle 4 has been reported elsewhere (20–22). Fig. 2 illustrates the effect of temperature on the aromatic spectrum at 300 MHz. At 25°C, nine singlets from the Trp and His side chains are clearly discerned in the spectrum (Fig. 2 *A*) and have been numbered 1–9 according to their order of appearance following the chemical shift ppm scale (21). Singlet 2 overlaps at this temperature with one of the resonances from a Tyr phenol doublet. On raising the temperature to 55°C most resonances sharpen (Fig. 2 *B*), the overall spectral pattern remaining little affected so that the correspondence between resonances in spectra *A* and *B* can be unambiguously established. Noticeable are some broadening of singlet 6 and a reduction of its amplitude in spectrum *A* relative to spectrum *B*. The sample was subsequently heated to 70°C causing the spectrum to assume the characteristics of that of a random-coil polypeptide (not shown); after remaining 2 h at this temperature, the sample was allowed to cool back to ambient temperature and was filtered to remove insoluble material, presumably denatured kringle. The spectrum of the sample was then recorded at 55°C (Fig. 2 *C*). Although, as judged from the signals in the 6.5 to 7.5 ppm region, renaturation is only partial, resonances appearing between 5 and 5.5 ppm, which are characteristic tertiary structure probes and which in spectrum *C* do not overlap with any signal from a denatured species, indicate that a significant fraction of the thermally unfolded kringle has regained its native form (compare spectra *B* and *C*, Fig. 2). A similar behavior has been observed for the BASA complex of kringle 1 (19). From Fig. 2, it is clear that singlets 5, 6, and 8 can be identified as His H2 protons (21) since these are the only carbon-bound hydrogens in His and Trp side chains that exchange with solvent deuterium atoms (28, and references therein) and they have disappeared from spectrum *C*. These experiments suggest that, despite the long expo-

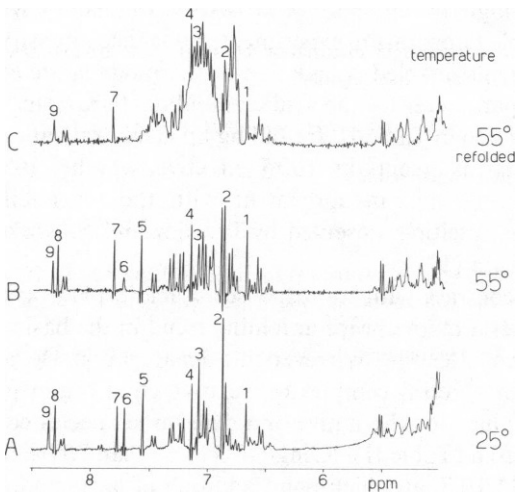

FIGURE 2 ^{1}H-NMR spectra of kringle 4: region low-field from the $^1H^2HO$ resonance at 298°K (*A*) and 328°K (*B*). Spectrum *C* was recorded at the same temperature as (*B*) after the kringle had been thermally unfolded at 343°K for 2 h. The kringle solutions were ~0.5 mM, in ^2H_2O pH* 7.2 The spectra were recorded at 300 MHz after exchange of labile hydrogen atoms for deuterium; each spectrum represents 4,000 scans.

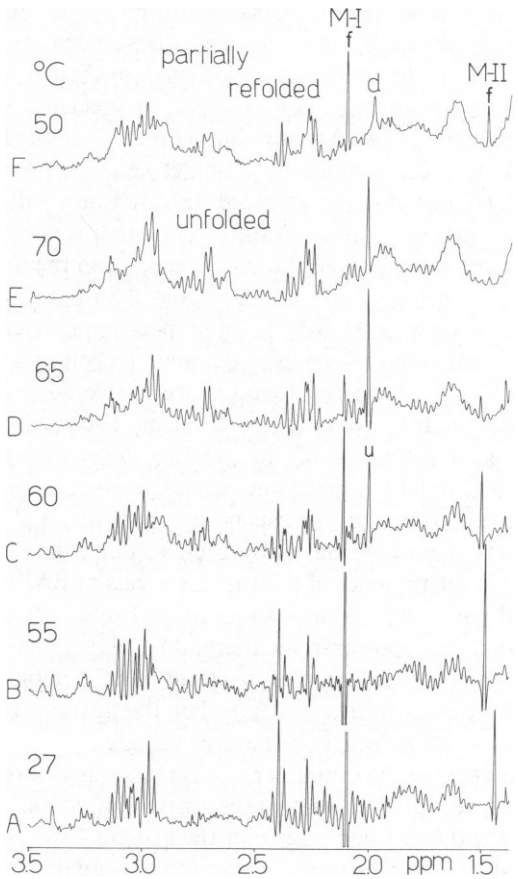

FIGURE 3 Effect of temperature on the ^{1}H-NMR spectrum of kringle 4 at 300 MHz: 3.5–1.5 ppm region. The S-CH_3^1 singlet resonances from the two methionyl residues are indicated as M-I and M-II for the protein in its native folded form (f); the same signals for the molecule in the unfolded state (u) overlap giving a single peak near 2.0 ppm and at ~1.96 ppm in the denatured species (d). The sample concentration is 0.5 mM in ^2H_2O, pH* 7.2. Each spectrum represents the average of 4,000 scans.

sure of kringle 4 to high temperature, the unfolded fraction that has not denatured refolds reversibly to the native structure, indicating that at temperatures moderate enough to preclude denaturation, folded and unfolded species freely interconvert in dynamic equilibrium. In our analysis, reversibility will be assumed, the validity of the assumption receiving support from our routine observation that kringle 4 heated to ~55–60°C recovers its native pattern ^{1}H-NMR spectrum upon cooling and from the agreement between our derived heats of unfolding and the calorimetric results (discussed below).

Fig. 3 *A* shows the 1.5–3.5 ppm region of the kringle 4 spectrum. Resonances from the six lysyl CH^{ε}_2 groups are centered ~3 ppm. Two Glu or Gln CH^{γ}_2 triplets are apparent at ~2.3 and 2.4 ppm. The S-CH^{ε}_3 singlets from the two Met residues at sites 28 and 48 (labeled M-I and M-II since as yet they have not been assigned to specific residues) are readily visible at 2.1 and 1.4 ppm. The latter is significantly shifted from the random coil position predicted for such a group (2.0–2.1 ppm). Successive temperature increases (spectra *B–E*) lead to progressive spectral changes. Between ~55°C and ~70°C folded and unfolded species coexist, as demonstrated by the separate signals exhibited by those groups whose chemical shift difference for the two states is larger than their interconversion exchange rate. For example, in spectrum *C*, the singlets from the two Met residues (I and II) in the folded state, f, are accompanied by a singlet near 2.0 ppm from the S-CH^{ε}_3 groups in the unfolded state, u. Similar duplications of signals are apparent for several other well-resolved resonances, among them those that arise from the methyls of Val^{-2} and from Val^{87} at ~0.98 and 0.85 ppm, respectively (not shown). At 70°C (*E*) the spectrum is essentially that of a random-coil polypeptide; upon recooling down to 50°C (*F*) native spectral features are recovered, which is also seen in the aromatic spectrum as discussed above. Thus, good estimates of the relative concentrations of folded and unfolded species at various temperatures could be derived from the corresponding spectral amplitudes. These measurements have also been accomplished for the kringle in the presence of a 2:1 molar excess of BASA. The derived parameter values are listed in Table I. It can be estimated that upon extreme thermal unfolding and subsequent cooling the samples back to 50°C, refolding is essentially quantitative (>90%) when the ligand is present but only ~50% effective for the free kringle.

In analogy to the kringle's response to temperature rises, lowering the pH* leads to progressive unfolding. Fig. 4 shows the 0.5–2.1 ppm region of the kringle 4 spectrum at selected pH* values in the acidic range: signals from the same groups in different conformational states (unfolded/folded) are well resolved. The geminal methyl doublets from the C-terminal Val^{87} in the less abundant species of kringle 4 (20) appear, at pH* ~4, as a false triplet near 0.85 ppm. At pH* 3.3 the triplet resolves into two doublets while signals from the same groups in the unfolded state

TABLE I
EQUILIBRIUM PARAMETERS FOR THE THERMAL UNFOLDING OF KRINGLE 4

T (°K)	Kringle 4		1:2 Kringle 4/BASA	
	[u]/[K4]	$\Delta G^{\circ *}_u$	[u]/[K4]	$\Delta G^{\circ *}_u$
323	0	—	0	—
328	0.06	7.23	0	—
333	0.35	1.75	0.013	11.98
338	0.78	−3.47	0.10	6.31
343	0.95	−8.51	0.49	0.12
348	1	—	0.84	−4.80
>353	1	—	1	—

The listed values result from resonance intensity measurement on selected resonances in the ^{1}H-NMR spectra of kringle 4, both free and in the presence of a twofold molar excess of BASA, as explained in the text; pH* = 7.2.
*$\Delta G^{\circ}_u = -RT\ln K_u$ in kJ · mol^{-1}.

start growing at slightly higher fields. At pH* 2.9 the two sets of resonances have nearly the same intensity, as manifested in the appearance of the symmetric multiplet near 0.9 ppm, whereas at lower pH* values, the signals from the unfolded form prevail. A similar pattern is observed for the NH_2-terminus Val^{-2} methyl doublet at 1 ppm. Regarding methionyl residues, the Met-I intensity decreases progressively for the folded form, while for Met-II the loss of intensity is accompanied by a shift and line broadening that most likely reflects titration of a neighboring carboxyl group (30). However, in contrast with what is observed for thermal unfolding (Fig. 3), we notice that the two Met S-CH^{ε}_3 singlets in the unfolded form (u) at 2 ppm are not degenerate, being resolved into two lines (Fig. 4 *F*). Similar changes are seen in spectra of the kringle in the presence of BASA. In analogy with the variable temperature experiment, resonance intensity measurements enabled calculation of thermodynamic equilibrium parameter for the acidic unfolding. Parameter values are quoted in Table II. Refolding upon neutralization from low pH* is essentially 100% effective, whether BASA is present or not, in agreement with the reversibility of thermal melting, observed by Privalov and co-workers, at acidic pH (17).

In contrast with its response to acidic pH*, kringle 4 exhibits a more abrupt unfolding trend in the basic range, eventually leading to irreversible denaturation. Despite the gain in spectral complexity, relative equilibrium population values for the native and denatured species could be measured (Table II). Kringle 4 is more than 70% native up to pH* 10.7, at which point addition of large amounts of base (KO^2H) are required to further raise the pH*, the solution becoming cloudy while yielding a characteristic sulphurous odor. When ^2HCl was added to neutralize the solution, a curdy precipitate developed. Presence of BASA shifts the denaturation profile higher by about 1 pH* unit (Table II). Already at pH* 9, the most sensitive probes for

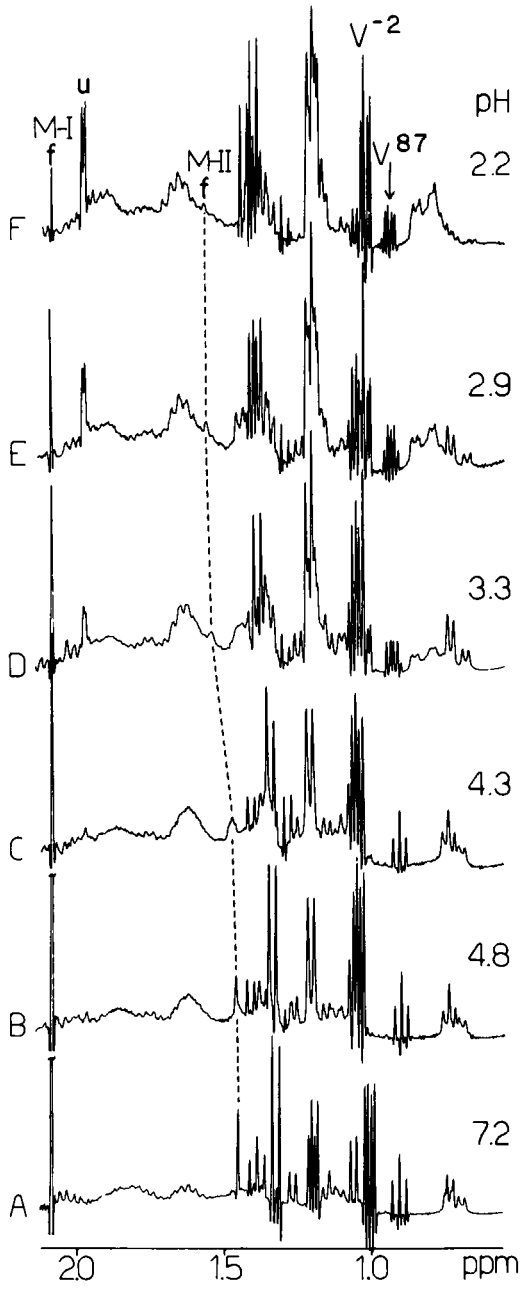

FIGURE 4 Effect of pH* on the ^{1}H-NMR spectrum of kringle 4 at 300 MHz: 0.5–2.0 ppm region. Methionyl singlets are labeled I and II as in Fig. 3; V^{-2} indicates the two geminal methyl doublets from the NH_2-terminal valine. V^{87} denotes the two methyl doublets from the COOH-terminal valine of -Ala^{85}-Ser^{86}-Val^{87}-COOH kringle 4 present in a relatively lesser amount than the predominant -Ala^{85}-COOH species. In contrast with the variable temperature experiment (Fig. 3), the Met S-CH_3^1 singlets in the unfolded species (u) give rise to two distinct signals. The kringle solution is 1 mM in ^2H_2O, 298°K; the spectra result from 3,000 scans each.

assessing presence of the kringle 4/BASA complex, such as several of the kringle's aromatic resonances (20), start to shift back towards their normal spectral positions in the absence of ligand. The BASA aromatic signals, too broad to be observed in the spectrum of the complex at the 1:2

TABLE II
EQUILIBRIUM PARAMETERS FOR THE ACID-BASE UNFOLDING OF KRINGLE 4

pH*	Kringle 4		pH*	1:2 Kringle 4/BASA	
	[u]/[K4]	ΔG_u^{o*}		[u]/[K4]	ΔG_u^{o*}
1.46	0.96	−8.15	—	—	—
1.95	0.88_5	−5.04	—	—	—
2.24	0.76	−2.91	—	—	—
2.59	0.63	−1.30	—	—	—
2.90	0.49	0.10	2.71	0.14	4.48
3.30	0.21	3.22	3.04	0.06	6.79
3.57	0.11	5.13	—	—	—
3.80	0.07	6.51	—	—	—
3.97_7	0.03_8	8.04	—	—	—
4.37–9.00	~0	—	3.51–9.50	~0	—
9.35	0.04_9	7.43	—	—	—
9.69	0.08_6	5.83	9.71	0.00_5	13.07
10.01	0.17_1	3.90	10.08	0.01_5	10.33
10.33	0.26_6	2.51	10.37	0.01_9	9.74
10.54	0.30_4	2.05	10.56	0.02_8	8.76
10.70	0.35_5	1.47	10.85	0.06_8	6.46
10.80	0.51_0	−0.10	11.05	0.11_5	5.04
11.00	0.95_4	−7.49	11.30	0.22_3	3.08
—	—	—	11.55	0.77_8	−3.10

The listed values result from intensity measurements on selected resonance in the ^{1}H-NMR spectra of kringle 4, both free and in the presence of a twofold molar excess of BASA, as explained in the text; T = 298°K. $^*\Delta G_u^{o*} = -RT\ln K_u^+$ in kJ · mol^{-1}

kringle 4/BASA ratio (20, 21), begin to emerge up from the kringle aromatic spectral background near pH* 10.5, i.e., just before the start of chemical denaturation. Similarly, in the acidic pH range, BASA signals at 7.6 ppm start showing at pH* ~4.7, further acidification causing the signals to sharpen and move low field towards their frequencies in the free-ligand spectrum.

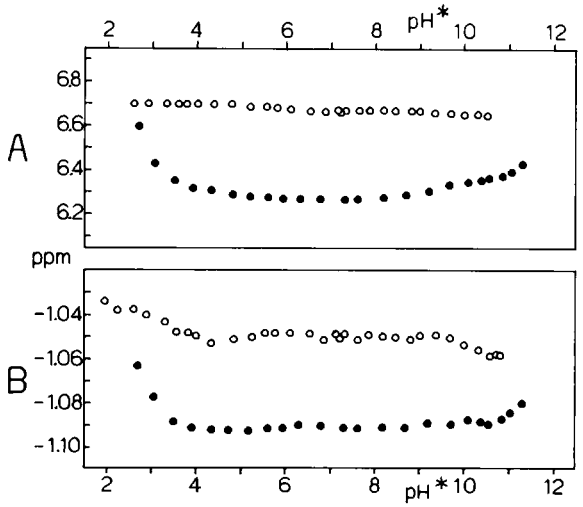

FIGURE 5 pH* dependence of chemical shift for selected resonances in the ^{1}H-NMR spectra of kringle 4 (○) and 1:2 kringle 4/BASA complex (●) at 300 and 600 MHz, respectively. (*A*) H2 indole singlet from Trp^{72}; (*B*) highest field δ-methyl doublet from Leu^{46}.

As observed in the basic pH range, kringle signals that are strongly displaced in the complex shift back upon acidification to the positions they display in the unligated species, the whole spectrum progressively evolving towards the free kringle pattern. For example, Fig. 5 shows the pH* dependence of chemical shift for the Trp^{72} H2 indole singlet (*A*) and for the high field methyl doublet from Leu^{46} (*B*) (21). Trp^{72} is particularly informative since its resonances are significantly shifted by addition of ligand (20, 21), the integrity of site 72 being crucial for complex formation (31). Leu^{46} methyl resonances, on the other hand, are not only affected by BASA (21) and other ligands, but they also appear in spectra of human plasminogen kringle 1 (19) and of bovine prothrombin kringle-containing fragments (32, 33), indicating that such a residue (and its local environment) is critical to the structure of the kringles' hydrophobic core (30). Fig. 5 shows that the kringle 4/BASA complex is stable within the acidity range $4 \lesssim pH^* \lesssim 10.5$. Outside this range, ligand is released and the unfolded species eventually predominates.

In the absence of ligand, kringle 4 denatures sharply and irreversibly between pH* 10.5 and 10.7. Thus, it is interesting to notice that in the presence of BASA, at pH* 11.3, the kringle 4 spectrum is essentially that of the native ligand-free species rather than that of its BASA complex. On the other hand, although the ligand/protein ratio is 2:1,

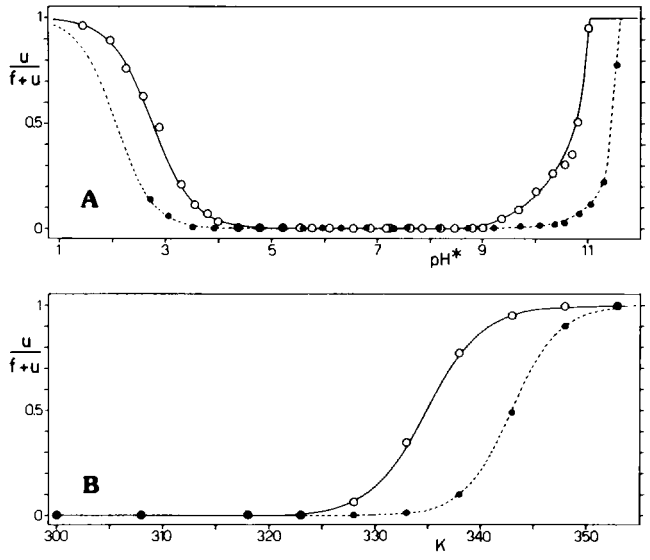

FIGURE 6 Plots of molar fraction of unfolded kringle 4. (*A*) pH dependence and (*B*) temperature dependence, for kringle 4 both in the absence (O) and in the presence (●) of twofold molar excess of BASA (see text, Tables I and II). The solid lines in *B* correspond to Eq. 2, where the ΔG_u° values, with and without ligand, are those reported in the text. In *A*, the solid and the dotted lines below pH* 5 obey Eq. 6 where the *s* and pH_u values, in the presence and in the absence of ligand, are those reported in Table V. The line for the BASA complex in the acidic range is dotted, as it was extrapolated from a linear fitting based on two points only. In the basic range, the lines are free interpolations between the data points, as the experimental data reflect both reversible unfolding and denaturation (Table VI, Figs. 8 *B* and 9).

TABLE III
THERMODYNAMIC PARAMETERS FOR THE THERMAL UNFOLDING OF KRINGLE 4, pH* 7.2

	ΔH_u° (kJ · mol^{-1})	ΔS_u° (J · mol^{-1} · K^{-1})	T_u (°K)
Kringle 4	349.8	1046	334.8
Kringle 4/BASA 1:2	389.1	1133	343.5

the BASA resonances are not yet sharp enough to be detected (20). Indeed, only at pH* ~11.5 do these signals become apparent, although quite broad. Since at pH* 11.3 the chemical shifts are those of unbound kringle 4, we tentatively conclude that at the two pH* extremes, i.e., under conditions that disfavor complex formation, BASA still interacts with the kringle, but with such low binding affinity that the NMR spectrum detects the kringle as mostly free ($k_{off} \gg k_{on}$). This suggests a pH dependence of the kringle 4/BASA complex dissociation rate constant, k_{off}. So, at high pH*, even if the ligand is mostly dissociated, it still confers significant protection to the kringle against alkaline denaturation.

The unfolding equilibrium constant K_u = [u]/[f] was extracted directly from the spectra recorded under the various conditions, as explained above. The temperature-dependence of the molar fraction [u]/[K4] is shown in Fig. 6 *B*. From linear-fitting the data in Table I to the Van't Hoff Eq. 1 we obtain the results found in Table III, where $T_u = \Delta H_u^\circ/\Delta S_u^\circ$, the unfolding temperature, is defined as the temperature at which folded and unfolded states are equally populated, i.e., for $\Delta G_u^\circ = 0$. Experimental data points and fitting curves are shown in Fig. 6 *B* (nonlinear, [u]/[K4] vs. *T*), and Fig. 7 (linear, $R\ln K_u$ vs. $10^3/T$). From the thermodynamic parameters at pH* 7.2 we calculate $\Delta G_u^\circ(298)$ = 38.1 kJ.mol^{-1} without BASA, $\Delta G_u^\circ(298)$ = 51.5 kJ.mol^{-1} with BASA.

With regard to the pH* response, the kringle 4 population ratio [u]/[K4] exhibits a single titration curve in the acidic range (Fig. 6 *A*) which can be well represented by the modified Henderson-Hasselbach Eq. (Eq. 4). Because of sample limitations, titration of the BASA complex could

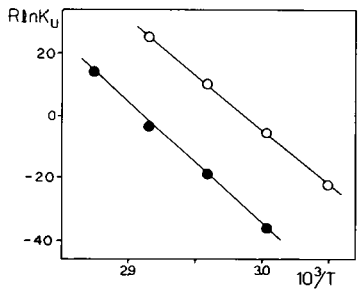

FIGURE 7 Temperature dependence of the equilibrium constant for the unfolding of kringle 4 (O) and of kringle 4 in the presence of BASA (2:1 ligand/kringle 4) (●). Straight lines result from the numerical fits discussed in the text. The units are $J \cdot K^{-1} \cdot mol^{-1}$ (ordinate) and $10^3 K^{-1}$ (abscissa).

TABLE IV
PARAMETERS FOR THE ACIDIC UNFOLDING OF KRINGLE 4, 298°K

	pH_u^+	s
Kringle 4	2.76	1.11
Kringle 4/BASA 1:2	2.07	1.23

TABLE V
PARAMETERS FOR THE BASIC UNFOLDING OF KRINGLE 4, 298°K

	pH_u^+	s
Kringle 4	11.0	0.79
Kringle 4/BASA 1:2	11.9	1.07

not be completed in the acidic range; hence Eq. 7 was fitted using the available experimental data and extrapolated to low pH*, yielding the curve indicated by a dashed (---) line in Fig. 6 *A*. From fitting the data for kringle 4 and for the kringle 4/BASA complex (Table II) to Eq. 8 we derive for the unfolding at low pH* the data found in Table IV. The fact that $s \gtrsim 1$ is probably related to the stoichiometry of proton dissociation, assumed, for simplicity, to be a one-proton process. Linear plots of ln K_u vs. pH* in the acidic range are shown in Fig. 8 *A*.

The data in Fig. 6 *A* indicate a relatively more complex process in the basic range. The corresponding plot of ln K_u vs. pH* (Fig. 8 *B*) shows that for both free kringle 4 and its BASA complex, the points lie on a straight line up to pH* ~10.7 for the former and ~11.3 for the latter, at which pH* values the lines break. We interpret such abrupt changes in the slope at high pH* as a reflection of base-catalyzed, irreversible denaturation (dotted segments in Fig. 8 *B*). The highest pH* data points were neglected in the linear fit (solid lines in Fig. 8 *B*) which, therefore, should yield pH_u^* estimates in the absence of denaturation. From the linear fittings indicated in Fig. 8 *B* we obtain, for the high-pH unfolding the values in Table V. The pH_u^* values, 11.0 without ligand and 11.9 in the presence of BASA, indicate a stabilizing effect of the ligand against the high-pH unfolding as well as ligand protection of the kringle against the concomitant irreversible alkaline denaturation.

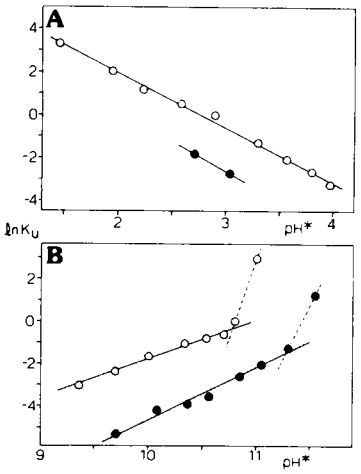

FIGURE 8 pH* dependence of the equilibrium constant for reversible unfolding of kringle 4 (O) and of kringle 4 in the presence of 2:1 excess ligand (●) in the acidic (*A*) and in the alkaline range (*B*). Straight lines result from the linear fitting discussed in the text. The dotted segments in *B* represent irreversible, chemical denaturation which dominates the unfolding at high pH* for both the intact and the complexed kringle.

Straight lines from fitting ΔG_u° vs. pH* in the acidic and basic ranges meet at near neutral pH* (Fig. 9). This might be relevant from a physiological standpoint, as it suggests maxima for ΔG_u° between pH* 6 and 7 for both the BASA complex and the intact kringle. From Fig. 9 we estimate $\Delta G^\circ_{u\max} \sim 21$ kJ.mol^{-1} for the free species and approximately 31.4 kJ.mol^{-1} in the presence of ligand. These values are significantly lower than the corresponding 38.4 kJ.mol^{-1} and 51.5 kJ.mol^{-1}, derived from the thermal unfolding ΔH_u° and ΔS_u° values at 298°K and pH* 7.2. This would suggest that the latter ΔG_u° is not linear over the full temperature range, probably decreasing in slope near physiological temperatures. Indeed, temperature-dependent ΔH_u° and ΔS_u° have been observed in several proteins (18).

Because the macroscopic protein unfolding can represent stability changes at a more local or microscopic level, the NH ^{1}H-^{2}H exchange was monitored to probe into dynamic aspects of the kringle structure (29, 34–36). Neglecting NH groups that overlap with the aromatic CH signals, we were able to follow the exchange for 19 protons both in kringle 4 and in the kringle 4/BASA complex. Fig. 10 shows 600 MHz spectra, recorded at various times after dissolving the sample, that illustrate the ^{1}H-^{2}H exchange both for kringle 4 and for the 2:1 kringle 4/BASA complex at pH* 7.2, 298°K. Monitored resonances are labeled in spectra 10 *A* (kringle 4 alone) and 10 *A'* (kringle 4/BASA complex), where a dot (•) is used to denote those reso-

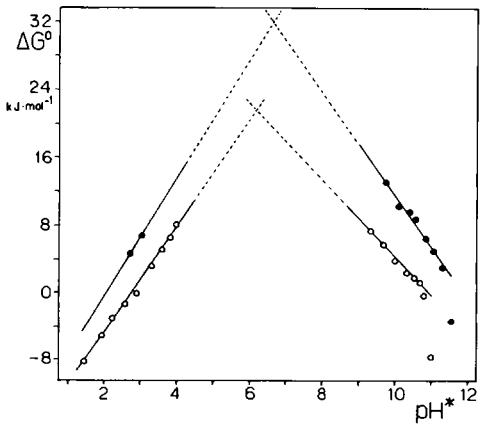

FIGURE 9 Plots of ΔG_u° vs. pH* for the unfolding of kringle 4 (O) and of kringle 4 in the presence of BASA (2:1 ligand/kringle) (●). Straight lines results from the linear fittings discussed in the text.

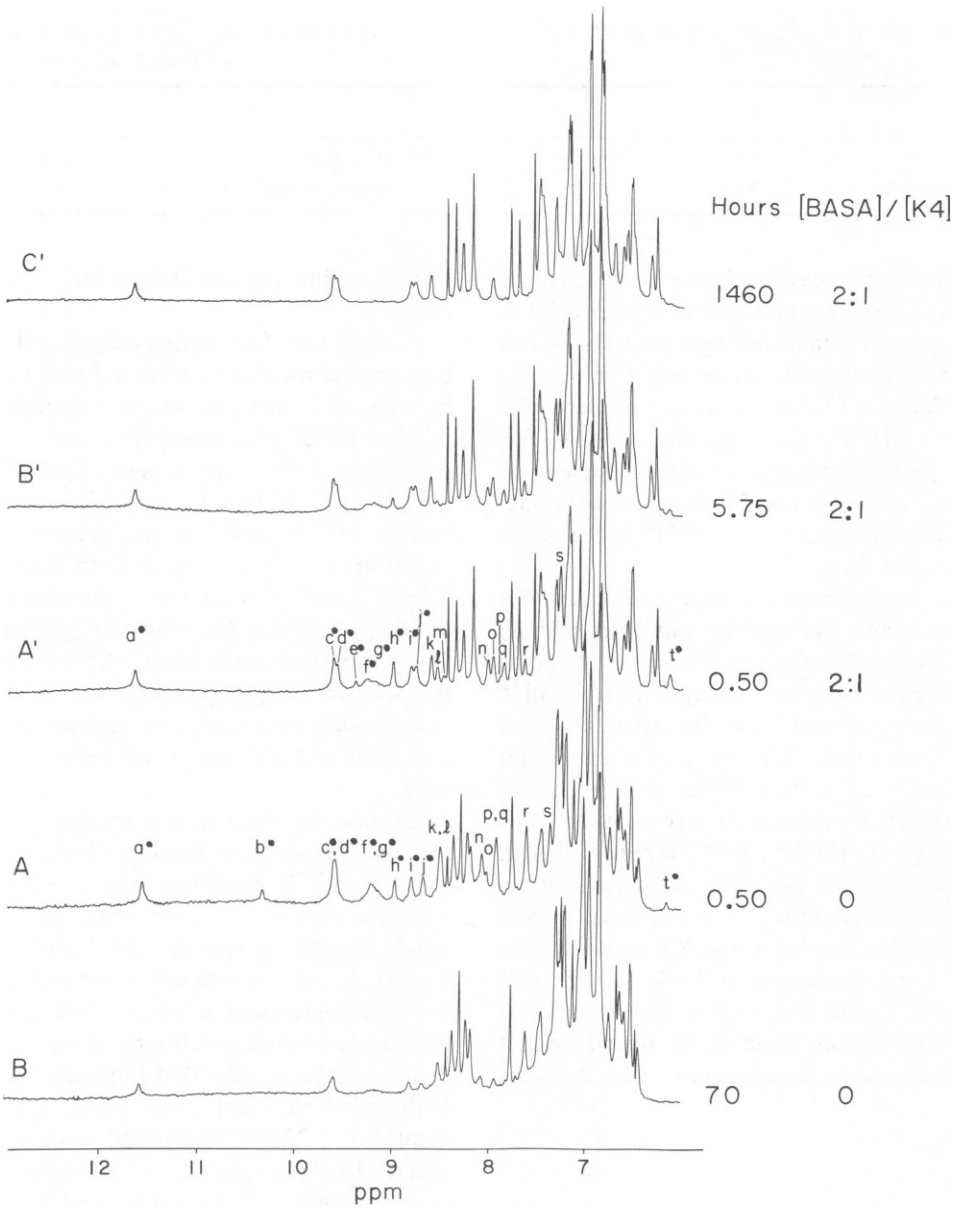

FIGURE 10 ^{1}H-NMR spectra of kringle 4 at 600 MHz: Effect of BASA on the hydrogen exchange kinetics. ^{1}H-^{2}H exchange has been followed for kringle 4 ligand free (spectra *A* and *B*) and for kringle 4 in presence of 2:1 BASA (spectra *A'*, *B'* and *C'*). Peaks are labeled in spectra *A* and *A'*, a dot (●) is used to indicate peaks of reasonably certain correspondence between the sample without ligand (spectrum *A*) and with ligand (spectrum *A'*). The kringle solutions were 1.2 mM, in ^2H_2O, pH* 7.2, 298°K. Each spectrum is an average of 1,200 scans.

nances whose correspondence between the two spectra appears reasonably unambiguous. After 70 h, most kringle 4 NH's have exchanged, only few of them remaining in the spectrum (Fig. 10 *B*). In fact, most of the slowest exchangeable protons in kringle 4 exhibit half-lives within this time range (Table VI). Interestingly, presence of BASA increases the average $t_{1/2}$ to almost 3 mo (Fig. 10 *B'* and *C'*, and Table VI). Semilogarithmic linear plots of three selected NH resonance amplitudes vs. time are shown in Fig. 11 for both kringle 4 (open symbols) and the kringle 4/BASA complex (filled symbols). In all these cases there is a consistent decrease in the exchange rates. The slowing down of the exchange rates is better appreciated by considering the retardation, defined as the ratio of $t_{1/2}$ for kringle in presence of ligand to that in absence of ligand (Table VI). Out of 19 resonances, 14 show a retardation >1, indicating that ~74% of the monitored protons experience a reduction in the exchange rate. Some of them (a•, c•, i•, j•, and k) undergo a retardation $\gtrsim 10^2$. In particular, resonance a• at ~11.6 ppm, which arises from the Trp I (Trp^{25} or Trp^{62}) indole NH hydrogen atom, shows a retardation of 1.69×10^2, thus revealing that, depending on the NH location, the protection of BASA against exchange can be dramatic.

TABLE VI
KINETIC PARAMETERS FOR ^1H-^2H EXCHANGE OF KRINGLE 4 NH PROTONS

NH*	$t_{1/2}$ (hours) Kringle 4	$t_{1/2}$ (hours) Kringle 4/BASA	Retardation‡	$\delta\Delta G\dagger$§ (kJ · mol^{-1})
a•	61.61	1.04×10^4	1.69×10^2	12.73
b•	0.60	<0.30	<0.50	<−1.73
c•	18.02	8.35×10^3	4.62×10^2	15.22
d•	37.00	3.48×10^3	94.05	11.26
e•	<0.13	1.72	>13.23	>6.39
f•	14.33	4.50	0.31	−2.90
g•	37.00	65.32	1.77	1.41
h•	3.89	4.48	1.15	0.34
i•	72.43	8.64×10^3	1.19×10^2	11.85
j•	60.11	9.64×10^3	1.60×10^2	12.58
k	10.74	1.23×10^3	1.15×10^2	—
l	87.96	3.48	3.96×10^{-2}	—
m	<0.13	3.50	>26.90	—
n	44.76	11.53	0.26	—
o	5.17	181.45	35.10	—
p	7.22	0.46	6.37×10^{-2}	—
q	22.77	6.83	0.30	—
r	11.22	36.29	3.23	—
s	73.75	19.44	0.26	—
t•	1.26	2.95	2.34	2.10
average:	28.51	2.10×10^3	60.23	6.30

Table VI shows exchange data for kringle 4 both free and in presence of a twofold molar excess of BASA.

*From resonances labeled according to Fig. 10. Dot (•) is used to denote resonances thought to correspond in spectra with and without ligand. Resonances c• and d•, f• and g•, and k and l, overlap pairwise in the spectrum of the free kringle and become resolved in the presence of ligand; their exchange kinetics was estimated by fitting two exponentials to the resonance amplitude decay.

‡Defined as the ratio of $t_{1/2}$ for the kringle in presence of ligand (column 3) to that in absence of ligand (column 2). For overlapping resonances c• and d•, f• and g•, and k and l, the retardations are calculated on the assumption of correspondence, as indicated; however, the correspondence is ambiguous in that the two resonances overlap in absence of ligand.

§$\delta\Delta G\dagger$ calculated using Eq. 9 for those resonances whose correspondences in spectra with and without ligand are confidently established.

In a previous paper (20) we have reported that at pH* 6.5, 1 mM, free kringle 4 exchanges all the NH's within ~40 h, while in this study we observe that at the same temperature (~298°K), pH* 7.2, 1.2 mM, the exchange takes place within about one week. This difference might arise from either a pH effect or concentration-dependent aggregation effects on the exchange rates or both. In the case of ferrichrome cyclohexapeptides we have suggested that the observed slow NH exchange at neutrality results from a gain in conformational stability bought about by stronger metal ion binding at pH 7 so that despite the well-known base catalysis of the amide H-exchange (29, 34–36) a relative retardation of the exchange kinetics can result (36, 37, and references therein). Thus, given that the kringle 4 structural stability is pH dependent (Fig. 6 *A*), it is difficult to predict the way structural fluctuations will be affected by a 0.7 pH* unit shift. At this point, we do not attribute much significance to this discrepancy since the fact remains that there is a major difference in the exchange rate between kringle 4 and its BASA complex.

The change in the Gibbs free energy of activation for the ^1H-^2H exchange owing to presence of the ligand was calculated from the equation

$$\delta\Delta G^{\dagger} = -RT \ln k_{K4/B}/k_{K4}, \qquad (9)$$

where T = 298°K, and $k_{K4/B}$ and k_{K4} are the first-order kinetic constants determined for a single resonance in presence and in absence of BASA, respectively. $\delta\Delta G^{\dagger}$ can be interpreted as a measure of the stabilization conferred by the ligand to a local microenvironment against solvent accessibility. It is interesting to observe that the averaged $\delta\Delta G^{\dagger}$ for all the studied protons is 6.30 kJ.mol^{-1}, which, when compared against the average $\Delta G^{\dagger}$ = 17.25 kJ.mol^{-1} obtained from the values reported by Privalov and Tsalkova (23) for the microunfolding of ligand-free proteins, suggests ~40% average increase in the height of the activation barrier for proton exchange. It must be noticed, however, that the NH's do not all respond to the same extent to the presence of ligand. In fact, the $\delta\Delta G^{\dagger}$ values for the stabilized protons range between 0.34 and 15.22 kJ.mol^{-1}, while two of them, b• and f•, yield $\delta\Delta G^{\dagger} < 0$, pointing to a local destabilization against exchange.

DISCUSSION

The present investigation indicates that BASA-binding induces on kringle 4 a T_u shift of ~9°K (Fig. 6 *B*). This result should be compared with the calorimetric studies of Castellino and co-workers (15) who, while characterizing the profile of thermal unfolding for kringle 4 at pH 7.4, determined ΔH = 364 kJ.mol^{-1} with a midpoint transition temperature T_m = 331.1°K. These values are in excellent agreement with the Van't Hoff ΔH_u° = 350 kJ.mol^{-1} and T_u = 334.8°K we determine at pH* 7.2, in ^2H_2O, on the basis of the kringle 4 [u]/[K4] population equilibria at the various temperatures, which affords strong support for the two-state model (18). In the presence of excess levels of ϵ-aminocaproic acid, Castellino and co-workers determined ΔH = 339 kJ.mol^{-1} and T_m = 344°K, suggesting little effect of the ligand on the enthalpy barrier but significant protection by ϵ-aminocaproic acid of the kringle 4 structure against thermal unfolding in that T_m is raised by ~12°K, which is also consistent with our observations regarding the effect of BASA on T_u. However, for the latter experiment we estimate an increase in ΔH_u of ~40 kJ.mol^{-1} upon BASA binding. Although it is also conceivable that vis-à-vis ϵ-aminocaproic acid BASA might exhibit a more pronounced ΔH_u° effect as a reflection of a stronger association with the kringle, it is also quite likely that the apparent insensitivity of the transition ΔH towards ϵ-aminocaproic acid reflects the relatively large experimental uncertainties inherent in the differential scanning calo-

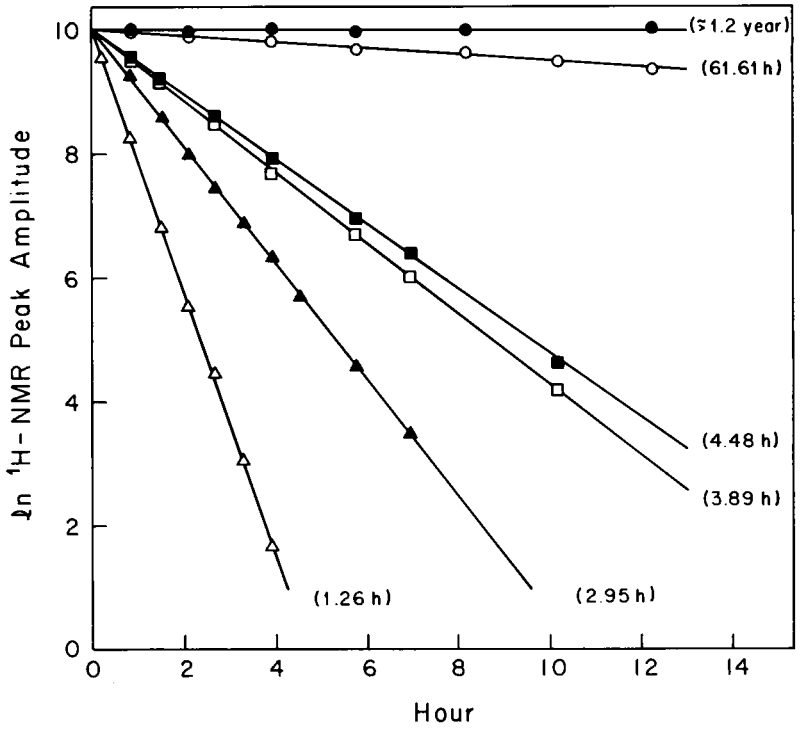

FIGURE 11 Plots of ln ^{1}H-NMR peak amplitude vs. time for selected NH resonances in spectra of kringle 4 in absence (open symbols) and in presence (filled symbols) of twofold molar excess of BASA. Circles (○, ●) correspond to peak a*; squares (□, ■) to peak h*; and triangles (△, ▲) to peak t* (refer to Fig. 10, spectra *A*, *A'*). The straight lines are least squares fits assuming a first-order decay and giving the same weight to each point. Numbers in parenthesis indicate half-decay times ($t_{1/2}$) for exchange in ^2H_2O, pH* 7.2, 298°K.

rimetry method, estimated to be about ±18% (15). Indeed, the T_u shift from 334 to 343°K resulting from complexation with BASA (Fig. 6 *B*) is mainly a result of ΔH_u° increasing since ligand-binding also rises ΔS_u° from 1,046 to 1,133 $J.K^{-1}.mol^{-1}$. Our results are also in excellent agreement with the more recent investigations of Privalov and collaborators (17) who observe a shift of the calorimetric transition temperature from 339.0 to 348.7°K upon ϵ-aminocaproic acid binding to kringle 4 at pH 8.0.

BASA binding also results in a pH_u^* shift of ~0.7 pH* units in the acidic range, and comparable or even larger shifts in the basic range (Fig. 6 *A*). BASA itself is titratable and amphoteric, the pK_a of related model compounds being 9.3 for benzylamine and 0.7 for benzosulfonic acid (38). However, within the pH range of stability of the complex there should be no influence from protonation of the ligand since in the acidic range the complex becomes destabilized much before the $-SO_3^-$ group titration occurs. In the basic range the complex is still present at pH values at which deprotonation of the free BASA $-NH_3^+$ group ought to occur. Therefore, it would appear that collapse of the kringle/BASA complex and unfolding of the kringle occur sequentially at the two extremes of pH: The level of the complex has to drop significantly before start of acid-base denaturation. A different pattern characterizes the thermal unfolding. At 70°C, pH* 7.2, such NMR probes as the high-field Trp^{72} indole H2 singlet and the adjoining Trp-II indole H6 triplet (39) remain with their full BASA-complex spectral characteristics (chemical shifts and intensities) although unfolding has already commenced. Indeed, BASA resonances do not sharpen unless denaturation is reached. Thus, in contrast with what is observed for the acid/base process, during the high-temperature unfolding the ligand does not dissociate significantly from kringle 4, which suggests that the ligand-binding site is structurally coupled to a thermally stable core.

It is most interesting that the ligand-enhanced stability of the kringle structure is accompanied by a retardation of NH ^{1}H-^{2}H exchange. The change in the exchange Gibbs free energy of activation resulting from BASA-binding, $\delta\Delta G^\dagger$, ranges between approximately −3 and 15 $kJ.mol^{-1}$ which clearly indicates that the exchange-labile sites do not respond to the same extent to the presence of ligand. It is currently thought that the NH exchange kinetics reflect both static structural constraints (intramolecular H-bonding, steric hindrance, etc.) and conformational fluctuations about a predominant tridimensional structure (29, 34–36). As has been pointed out by Woodward and collaborators (35) the proposed mechanisms of NH exchange involve either local cooperative unfoldings or direct solvent penetration accompanying fast conformational fluctuations. To the extent that ligand-binding shifts both T_u and pH_u, it is clear that the ligand stabilizes the kringle 4 macrostruc-

ture. On the other hand, since from an NMR standpoint (Fig. 6 *A, B*) at 298°K, pH* 7.2, the domain architecture is well described by the native, fully folded conformation, much of the H-exchange retardation discussed above (Figs. 10 and 11) should be ascribed to effects that modulate the local dynamic microenvironment at the individual NH sites.

It might be argued that in the case of kringle 4 the ligand could interfere with the isotope exchange by blocking solvent accessibility of some groups; however, one would not expect such an effect to be a major one in view of the small size of a BASA molecule. On the other hand, recalling from previous ^{1}H-NMR studies that BASA does not cause significant changes of the kringle conformation (19, 21), one is led to conclude that the effect of ligand complexation is predominantly on the dynamics of the kringle. Since as probed by the ^{1}H-^{2}H exchange the effect is not uniform for all the NH sites, it is likely that in establishing salt bridges linking polar groups at its two extremes, probably with Asp^{57} and Arg^{71} (40), and plugging the lysine binding site by establishing Van der Waals contacts with a number of hydrophobic, mostly aromatic, side chains (19–22), the ligand assists in rigidifying local structures to various extents, depending on the way the strains propagate from the binding site to the rest of the polypeptide framework. This is analogous to the effect of metal binding on the conformational state of metalloproteins (37). In fact, the ligand affects mainly the NH groups that already are somewhat buried in the ligand-free kringle, which is in agreement with the idea that the microstability of a protein structure is determined by clusters of nonpolar residues in the protein interior (18, 23). In this context, it is most interesting that the partial specific heat capacity, defined as $\Delta_t C_p = \delta \Delta H_u^\circ / \delta T_u$, yields 0.452 J/g$K$ (=39.3 kJ.mol^{-1}/8.7 K/10,000 g.mol^{-1}) for the kringle 4-ligand interaction, a value that is typical of globular proteins and which has been interpreted by Privalov (18) to imply that unfolding involves exposure of a hydrophobic core.

Clearly, the experiments described in this paper do not warrant a more detailed interpretation given the complexity of the kringle 4/BASA system. More satisfactory explanations as to the mechanisms of ligand-induced stabilization of the kringles' structure will demand assigned NH resonances and an accurate measurement of the temperature and pH dependence of the H-exchange rates. In the meanwhile, a preliminary characterization of ligand effects on the plasminogen kringle 4 structure in terms of macro- and microstabilities criteria has been achieved.

This research was supported by the U. S. Public Health Service, National Institutes of Health grants HL-15535 and HL-29409. The 600 MHz NMR facility is supported by the U. S. Public Health Service, National Institutes of Health grant RR-00292.

Received for publication 11 December 1984 and in final form 29 April 1985.

REFERENCES

1. Wallén, P. 1979. Plasminogen and fibrinolysis. *In* Plasma Proteins. B. Blombaek, and L. A. Hanson, editors. John Wiley & Sons, Inc., Chichester. 288–304.
2. Marsh, N. 1981. Fibrinolysis. Chapter 2. John Wiley & Sons, Inc., Chichester. 18–45.
3. Castellino, F. J. 1981. Recent advances in the chemistry of the fibrinolytic system. *Chem. Revs.* 81:431–446.
4. Sottrup-Jensen, L., H. Claeys, M. Zajdel, T. E. Petersen, and S. Magnusson. 1978. The primary structure of human plasminogen: Isolation of two lysine-binding fragments and one "mini-"plasminogen (MW 38,000) by elastase-catalyzed-specific limited proteolysis. *Progr. Chem. Fibrinolysis Thrombolysis.* 3:191–209.
5. Wiman, B., H. R. Lijnen, and D. Collen. 1979. On the specific interaction between the lysine-binding sites in plasmin and complementary sites in α_2-antiplasmin and in fibrinogen. *Biochim. Biophys. Acta.* 579:142–154.
6. Thorsen, S., I. Clemmensen, L. Sottrup-Jensen, and S. Magnusson. 1981. Adsorption to fibrin of native fragments of known primary structure from human plasminogen. *Biochim. Biophys. Acta.* 668:377–387.
7. Winn, E. S., S.-P. Hu, S. M. Hochschwender, and R. A. Laursen. 1980. Studies on the lysine-binding sites of human plasminogen: The effect of ligand structure on the binding of lysine analogs to plasminogen. *Eur. J. Biochem.* 104:579–586.
8. Lerch, P. G., E. E. Rickli, W. Lergier, and D. Gillessen. 1980. Localization of individual lysine-binding regions in human plasminogen and investigations on their complex-forming properties. *Eur. J. Biochem.* 107:7–13.
9. Váli, Z., and L. Patthy. 1982. Location of the intermediate and high affinity ω-aminocarboxylic acid-binding sites in human plasminogen. *J. Biol. Chem.* 257:2104–2110.
10. Cole, K. R., and F. J. Castellino. 1984. The binding of antifibrinolytic amino acids to kringle 4-containing fragments of plasminogen. *Arch. Biochem. Biophys.* 229:568–575.
11. Magnusson, S., T. E. Petersen, L. Sottrup-Jensen, and H. Claeys. 1975. Complete primary structure of prothrombin: Isolation, structure and reactivity of ten carboxylated glutamic acid residues and regulation of prothrombin activation by thrombin. *In* Proteases and Biological Control. E. Reich, D. B. Rifkin, and E. Shaw, editors. Cold Spring Harbor Laboratory. 123–149.
12. Günzler, W. A., G. J. Steffens, F. Ötting, S.-M. A. Kim, E. Frankus, and L. Flohé. 1982. The primary structure of high molecular mass urokinase from human urine: The complete amino acid sequence of the A chain. *Hoppe-Seyler's Z. Physiol. Chem.* 363:1155–1165.
13. Pennica, D., W. E. Holmes, W. J. Kohr, R. N. Harkins, G. A. Vehar, C. A. Ward, W. F. Bennett, E. Yelverton, P. H. Seeburg, H. L. Heyneker, D. V. Goeddel, and D. Collen. 1983. Cloning and expression of human tissue-type plasminogen activator cDNA in *E. coli. Nature (Lond.).* 301:214–221.
14. Patthy, L., M. Trexler, Z. Váli, L. Bányai, and A. Váradi. 1984. Kringles: Modules specialized for protein binding. Homology of the gelatin-binding region of fibronectin with the kringle structure of proteases. *FEBS (Fed. Eur. Biochem. Soc.) Lett.* 171:131–136.
15. Castellino, F. J., V. A. Ploplis, J. R. Powell, and D. K. Strickland. 1981. The existence of independent domain structures in human Lys^{77}-plasminogen. *J. Biol. Chem.* 256:4778–4782.
16. Privalov, P. L. 1982. Stability of proteins which do not represent a single cooperative system. *Adv. Protein Chem.* 35:1–104.
17. Novokhatny, V. V., S. A. Kudinov, and P. L. Privalov. 1984. Domains in human plasminogen. *J. Mol. Biol.* 179:215–232.
18. Privalov, P. L. 1979. Stability of proteins: Small globular proteins. *Adv. Protein Chem.* 33:167–241.
19. De Marco, A., S. M. Hochschwender, R. A. Laursen, and M. Llinás. 1982. Human plasminogen: Proton NMR studies on kringle 1. *J. Biol. Chem.* 257:12716–12721.

20. Hochschwender, S. M., R. A. Laursen, A. De Marco, and M. Llinás. 1983. 600 MHz ^{1}H nuclear magnetic resonance studies of the kringle 4 fragment of human plasminogen. *Arch. Biochem. Biophys.* 223:58–61.
21. Llinás, M., A. De Marco, S. M. Hochschwender, and R. A. Laursen. 1983. A ^{1}H-NMR study of isolated domains from human plasminogen: structural homology between kringles 1 and 4. *Eur. J. Biochem.* 135:379–391.
22. Trexler, M., L. Bányai, L. Patthy, N. D. Pluck, and R. J. P. Williams. 1983. The solution structure of kringles: NMR studies on native and several chemically modified kringle 4 species of human plasminogen. *FEBS (Fed. Eur. Biochem. Soc.) Lett.* 154:311–318.
23. Privalov, P. L., and T. N. Tsalkova. 1979. Micro- and macro-stabilities of globular proteins. *Nature (Lond.).* 280:693–696.
24. Evans, G. W., and B. Milligan. 1967. Some unsymmetrically substituted thiourea derivatives. *Aust. J. Chem.* 20:185–188.
25. Ernst, R. R. 1966. Sensitivity enhancement in magnetic resonance. *Adv. Magn. Reson.* 2:1–135.
26. Ferrige, A. G., and J. C. Lindon. 1978. Resolution enhancement in FT NMR through the use of a double exponential function. *J. Magn. Reson.* 31:337–340.
27. De Marco, A. 1977. pH dependence of internal references. *J. Magn. Reson.* 26:527–528.
28. Markley, J. L. 1975. Observation of histidine residues in proteins by means of nuclear magnetic resonance spectroscopy. *Acc. Chem. Res.* 8:70–80.
29. Hvidt, A., and S. O. Nielsen. 1966. Hydrogen exchange in proteins. *Adv. Protein Chem.* 21:287–386.
30. De Marco, A., R. A. Laursen, and M. Llinás. 1985. Proton Overhauser experiments on kringle 4 from human plasminogen: Implications for the structure of the kringles' hydrophobic core. *Biochim. Biophys. Acta.* 827:369–380.
31. Hochschwender, S. M., and R. A. Laursen. 1981. The lysine-binding sites of human plasminogen. *J. Biol. Chem.* 256:1172–1176.
32. Esnouf, M. P., E. A. Israel, N. D. Pluck, and R. J. P. Williams. 1980. The study of bovine prothrombin fragments by high-resolution proton magnetic resonance spectroscopy. *In* The Regulation of Coagulation K. G. Mann and F. B. Taylor, editors. Elsevier/North-Holland, New York. 67–74.
33. Pletcher, C. H., E. F. Bouhoutsos-Brown, R. G. Bryant and G. L. Nelsestuen. 1981. Effects of temperature and pH on prothrombin fragment 1 conformation as determined by nuclear magnetic resonance. *Biochemistry.* 20:6149–6155.
34. Linderstrøm-Lang, K. 1955. Deuterium exchange between peptides and water. *Spec. Publ. Chem. Soc.* 2:1–20.
35. Woodward, C., I. Simon, and E. Tüchsen. 1982. Hydrogen exchange and the dynamic structure of proteins. *Mol. Cell. Biochemistry.* 48:135–160.
36. Englander, S. W., and N. R. Kallenbach. 1984. Hydrogen exchange and structural dynamics of proteins and nucleic acids. *Quart. Revs. Biophys.* 16:521–655.
37. Llinás, M. 1973. Metal-polypeptide interactions: the conformational state of iron proteins. *Struct. Bonding.* 17:135–220.
38. Weast, R. C., and M. J. Astle, editors. 1981. *CRC Handbook of Chemistry and Physics.* 62nd Edition. CRC Press Inc., Boca Raton, Florida.
39. De Marco, A., N. D. Pluck, L. Bányai, M. Trexler, R. A. Laursen, L. Patthy, M. Llinás, and R. J. P. Williams. 1985. Analysis and identification of aromatic signals in the proton magnetic resonance spectrum of the kringle 4 fragment from human plasminogen. *Biochemistry.* 24:748–753.
40. Trexler, M., Z. Váli, and L. Patthy. 1982. Structure of the ω-aminocarboxylic acid-binding sites of human plasminogen: Arginine 70 and aspartic acid 56 are essential for binding of ligand by kringle 4. *J. Biol. Chem.* 257:7401–7406.